Boundary layer separation in the surface quasi-geostrophic equations

A. BRACCO
Istituto di Cosmogeofisica - Corso Fiume 4, 10133 Torino, Italy

(ricevuto il 25 Ottobre 1999; revisionato il 18 Febbraio 2000; approvato il 21 Marzo 2000)

Summary. — Uniform potential vorticity flows are investigated. The evolution of surface potential temperature is studied in a two-dimensional oceanic model driven by a surface heating. The surface temperature plays the role of the vorticity, but the different relationship between the streamfunction and the advected scalar implies the formation of unidirectional free waves. Important distinctive features with respect to the standard homogeneous models are pointed out.

PACS 92.10.Lq – Physics of the oceans: turbulence and diffusion.
PACS 07.05.Tp – Computer modeling and simulation.

1. – Introduction

In the quasi-geostrophic system, flows with uniform potential vorticity reduce to the evolution of potential temperature or surface buoyancy on horizontal boundaries [1]. On these boundaries the vertical motion vanishes, but the horizontal temperature gradients are nonzero.

This work provides an application of surface quasi-geostrophic equations (SQG in the following) in a simple oceanic continuously stratified model with a tilted upper boundary. One of the most striking features of the oceanic circulation is the observed separation of western boundary current. It has been shown that many possible mechanisms can influence the separation of the west boundary current from the coast: boundary conditions (free or no slip) [2-4], bottom topography [5-9], the presence of an asymmetric component in the wind forcing [10], coastline orientation [11], inertia on the midlatitude jet [12], interaction with the deep western boundary current [13, 14].

In particular, the outcropping mechanism provides one of the simplest explanations of the separation of the western boundary current in wind-driven gyres of opposite signs [15-18]. Assuming that the effects of the friction and inertia are confined to regions of boundary layer character, the separation latitude is shown to depend on the degree of stratification [19]. Recent models of the wind-driven circulation in a closed basin solve the two-dimensional quasi-geostrophic or the shallow-water equations with layers outcropping and with vertical discretization in constant density layers: the separation latitude and the resulting circulation is strongly dependent on the choice of the stratification. Using the SQG equations we can study the problem of the separation

of western boundary currents in a continuously stratified model, where the outcropping of the interior flow can occur *continuously* and the separation latitude is not dictated by the choice of the vertical coordinate.

In this paper an application of the SQG dynamics to a simple ocean model is investigated. The SQG equations are presented in the following section. The analytical solution for the linear problem and the physical implications are discussed in sect. **3**. In sect. **4** we face up to the nonlinear problem and we show the results from numerical calculations based on the SQG system forced by a wind forcing pattern with a single- and double-gyre configuration. We compare these simulations with numerical solutions of a single-layer quasi-geostrophic model in a beta-plane basin. The discussion of the results is contained in the final section.

2. – Equations of motion: Surface Quasi-Geostrophic Dynamics

We consider the problem of 3-dimensional flows driven by the dynamics of upper boundary, the internal dynamics being the vanishing potential vorticity.

In the limit of small Rossby number ($R_0 = U/f_0 L \ll 1$), the quasi-geostrophic approximation of the equations of motion in the inviscid limit is (see [20] for a complete derivation)

$$\partial_t q = - J(\psi, q), \tag{1}$$

where $J(\psi, q)$ is the Jacobian operator, $(\psi_x q_y - \psi_y q_x)$, with the condition on the streamfunction of non-normal flow at a rigid horizontal boundary:

$$\partial_t \theta = - J(\psi, \theta), \qquad z = z_1, z_2 \tag{2}$$

(z_1, z_2 being the upper and the lower boundaries).

We assume that $q \equiv (\partial_{xx} + \partial_{yy} + \varrho_s \partial_z \varrho_s \varepsilon \partial_z)\, \psi$ is the 3-dimensional potential vorticity.

The streamfunction ψ represents the pressure field related to the horizontal velocity field in the usual way $(u, v) = (-\psi_y, \psi_x)$ and $\psi_z \equiv \theta$ is the potential temperature or surface buoyancy. ϱ_s is a function of z and may be defined as the density global average at each level z. ε is the inverse of the stratification parameter $S = S(z)$ and is defined by

$$\frac{1}{S(z)} = \varepsilon = \frac{f_0^2 L^2}{N^2 D^2}, \tag{3}$$

where $f_0/2$ is the Coriolis parameter, L is the characteristic horizontal length, D the vertical scale, $N(z) = \left(\frac{g}{\theta} \frac{\partial \theta}{\partial z} \right)^{1/2}$ is the Brunt-Väisälä frequency.

In the ocean, where the compressibility effect on the fluid element is negligible, the Brunt-Väisälä frequency is given in term of the equilibrium density distribution $N = \left(- \frac{g}{\varrho} \frac{\partial \varrho}{\partial z} \right)^{1/2}$ and the basic density field may be considered roughly constant.

Under this hypothesis the factor ε is subsumed into a rescaled vertical coordinate $z' = \varepsilon^{1/2} z$. (We will retain the notation z for the rescaled z'.)

A familiar special case of 3-dimensional flow is obtained by assuming $\theta = 0$, $z = z_1$, z_2. In this context the resulting flow is the so-called "Charney type" [21] or

quasi-geostrophic one, and the dynamical effect of the upper and lower boundaries are neglected. In other words, the flow is confined within isoentropic surfaces with uniform pressure and temperature. The complementary problem is the surface quasi-geostrophic flows, or flows of "Eady type" [22, 23], in which $q = 0$ is assumed. The interior equation (1) is identically satisfied and the flow is driven by the dynamics of upper and lower boundaries.

We are interested in this second case applied to an ideal ocean basin. In this approach it is assumed that the flow is confined in a closed horizontal basin with infinite depth, in the approximation of zero potential vorticity at the interior. Typical scales relevant to the North Atlantic Ocean are $U \sim O(2 \cdot 10^{-2}\,\mathrm{ms}^{-1})$, $L \sim O(10^3\,\mathrm{km})$, $f_0 \sim O(10^{-4}\,\mathrm{s}^{-1})$.

Introducing a tilted surface with elevation $z = -\lambda y$ in order to reproduce the beta-effect in 2-dimensional flows, the equations of motion take the form

$$
\begin{aligned}
\partial_t \theta &= -J(\psi,\, \theta - \Lambda y) + F, \qquad && z = 0\,, \\
\theta &\equiv \partial_z \psi\,, && \\
(\partial_{xx} + \partial_{yy} + \partial_{zz})\,\psi &= 0\,, \qquad && z < 0\,, \\
\psi_z &\to 0\,, \qquad && \text{as } z \to -\infty\,,
\end{aligned} \tag{4}
$$

where $\Lambda = \dfrac{\lambda N}{f_0 L R_0}$ is the nondimensional topographic variation and F is a given forcing function.

In terms of spectral amplitude, in a periodic domain with infinite depth for a 2-dimensional flow $\psi = Re[\widehat{\psi} \exp(ikx + iky - i\omega t)]$. The vertical structure which satisfies the system (4) is $\widehat{\theta} = (k^2 + l^2)^{1/2}\widehat{\psi}$ and supports linear waves travelling westwards with a dispersion relation

$$
\omega = -\frac{\Lambda k}{(k^2 + l^2)^{1/2}}\,. \tag{5}
$$

These waves decay away from the surface as $\exp[kz]$ and are dynamically identical to topographic edge waves.

3. – The linear problem

In order to show how the interior and the western boundary layers develop in a basin governed by the linear version of the SQG equations, we examine the free modes of the system for a general configuration with $0 \leqslant x \leqslant L$, $0 \leqslant y \leqslant L$ and $-B \leqslant z \leqslant 0$. The linear, nondimensional, inviscid equations are

$$
\begin{aligned}
q = \nabla^2 \psi = 0\,, &\quad 0 \leqslant x \leqslant L;\ 0 \leqslant y \leqslant L;\ -B < z < 0;\ t \geqslant 0\,, \\
\partial_t \psi_z - \Lambda \psi_x = 0\,, &\quad 0 \leqslant x \leqslant L;\ 0 \leqslant y \leqslant L;\ z = 0;\ t \geqslant 0\,, \\
\psi = 0\,, &\quad x = 0, L;\ y = 0, L;\ z < 0;\ t \geqslant 0\,, \\
\psi_z = 0\,, &\quad z = -B\,.
\end{aligned}
$$

Without loss of generality we can assume a periodic behaviour in the meridional direction by setting $\psi(x, y, z) = \phi(x, z) \sin(ly)$.

The system supports propagating waves solutions of the form

$$\phi = \mathrm{Im}\{A\cosh[(k^2+l^2)^{1/2}(z+B)]\exp[ikx - i\Lambda\omega t]\} \tag{6}$$

with the dispersion relation

$$\omega = -\frac{k}{(k^2+l^2)^{1/2}}\coth[(k^2+l^2)^{1/2}B]. \tag{7}$$

The phase speed in the x-direction is

$$C_{px} = -\frac{1}{(k^2+l^2)^{1/2}}\coth[(k^2+l^2)^{1/2}B] \tag{8}$$

and the two components of the group velocity are given by

$$\begin{cases} C_{gx} = -\dfrac{l^2\coth[(k^2+l^2)^{1/2}B]}{(k^2+l^2)^{3/2}} + \dfrac{Bk^2}{(k^2+l^2)\sinh^2[(k^2+l^2)^{1/2}B]}, \\ C_{gy} = -\dfrac{kl}{k^2+l^2}\left[\dfrac{\coth[(k^2+l^2)^{1/2}B]}{(k^2+l^2)^{3/2}} - \dfrac{B}{\sinh^2[(k^2+l^2)^{1/2}B]}\right]. \end{cases} \tag{9}$$

In the limit $B \to -\infty$, which represents a strongly stratified ocean, z scale as $\frac{fL}{N}z'$ and

$$\begin{cases} \omega \to -\dfrac{k}{(k^2+l^2)^{1/2}}, \\ C_{px} \to -\dfrac{1}{(k^2+l^2)^{1/2}}, \\ C_{gx} \to -\dfrac{l^2}{(k^2+l^2)^{3/2}}. \end{cases} \tag{10}$$

The phase speed and the group velocity along the horizontal axis are always negative. The waves are unidirectional: all the energy is transmitted westwards from the eastern boundary, while there is no possibility to propagate information eastwards. This behavior contrasts with the wave-like solutions for the planetary wave equation in a closed basin; in that case short waves carry energy from the western boundary and the inviscid system does not achieve a steady state [24].

In our model there is no reversal of group velocity for short waves, the linear unforced system develops a steady state in the interior and an infinite-time singularity along the western boundary. It is an open question whether a shock can form in SQG flow. Recently Constantin *et al.* [25] have shown that no finite time singularities occur in SQG flow with numerical methods combined with analytical criteria and there is no observation in favor of a finite-time singularity.

The waves in this limit are analogous to double Kelvin waves [26, 27]. Choosing the north-south wave number equal to one, it appears that long waves travel faster and both speeds decrease to zero with decreasing wavelength.

For the homogeneous model ($B \to 0$) the phase speed increases indefinitely with increasing wavelength and decrease to zero for short waves.

The free-wave solutions are analogous to solutions found by Johnson [28] and Johnson and Davis [29] for topographic waves which propagate with shallow water to their right (in the Northern Hemisphere) over a topography consisting of a single step-like escarpment bounded by a vertical sidewall. An unsteady, thinning boundary layer forms at the wall, there is no reversal of group velocity for short waves, the energy propagation is unidirectional and the energy carried towards the wall accumulates there. In [28] the free modes of the system are examined. In [29] the transient development of the steady flow combined with the development of the singularity near the wall-step junction is presented for the unforced and forced cases. A closed-form solution of the problem with a bounding wall (semi-infinite domain) is obtained using a Green's function for free-surface point vortices. The same method could be extended to our model in a finite domain.

4. – The nonlinear problem

In the following, we present the results from numerical integration of the fully nonlinear, time-dependent problem. Our model includes an explicit bottom friction term and a surface heating due to the wind stress. The lateral friction is supposed to be zero in order to minimize the influence of frictional boundary layers [30, 31].

It has been shown that the homogeneous model of the Ekman layer is valid for a stratified fluid [31], and the dominant contributions to the frictional forces in dimensional form can be rapresented as

$$\text{(11)} \qquad \begin{cases} \dfrac{A_v N^2}{f^2 L^2} \dfrac{\partial^2 u}{\partial z^2} = \dfrac{E_v}{2} \dfrac{\partial^2 u}{\partial z^2}, \\ \dfrac{A_v N^2}{f^2 L^2} \dfrac{\partial^2 v}{\partial z^2} = \dfrac{E_v}{2} \dfrac{\partial^2 v}{\partial z^2}, \end{cases}$$

where A_v is the vertical turbulent viscosity coefficient and E_v is the Ekman number associated with vertical mixing.

The forcing results from an applied heating $F = W \nabla \times \bar{\tau}$ and W in nondimensional coordinates is $\dfrac{\tau_0 N}{\varrho_s U^2 f}$ with the maximum wind stress value τ_0 on the order of $10^{-1}\,\mathrm{Nm}^{-2}$.

It is easy to verify that the linear time-independent problem for the SQG dynamics reduces to the system originally solved by Stommel [32] with the boundary condition that the coast has to be a streamline. The interior circulation satisfies the Sverdrup relation $\Lambda v = \nabla \times \bar{\tau}$ and the frictional boundary layer thickness is $\dfrac{E_v^{1/2}}{2R_0 \Lambda}$.

The equation

$$\text{(12)} \qquad \partial_t \psi_z + J(\psi, \psi_z - \Lambda y) = \frac{E_v^{1/2}}{2R_0} (\partial_{xx} \psi + \partial_{yy} \psi) + F$$

is integrated on a square basin of length 1000 km and infinite depth, with $\psi = \psi(x, y, 0)$ and free-slip boundary condition. The domain is smaller than a typical ocean basin (~ 4000 km), but allows for reaching a higher effective Rossby number, with a

better resolution of the inertial boundary layers and larger inertial gyres with respect to the basin size.

The other dimensional quantities of interest are $\varrho_s = 10^3\,\mathrm{kg\,m^{-3}}$ and $f_0 = 10^{-4}\,\mathrm{s^{-1}}$.

For a single anticyclonically forced subtropical gyre

$$\bar{\tau} = \left[W \cos\left(\frac{\pi y}{L}\,,\, 0 \right) \right] \tag{13}$$

and for an antisymmetrically forced double gyre

$$\bar{\tau} = \left[W \cos\left(\frac{2\pi y}{L}\,,\, 0 \right) \right], \tag{14}$$

giving a counterclockwise gyre north of the zero wind stress curl line (ZWCL) and an anticyclonically gyre to the south. This last configuration holds the formation of an intergyre boundary and a jet. The Sverdrup dynamics implies that the interior meridional drift must return in intense western boundary currents. These currents can be unstable and in the homogeneous model conditions for instability are easily verified in jet regions.

A finite-difference approximation of eq. (12) is integrated forward in time with a third-order Adams-Bashforth scheme from an initial state at rest on a square grid of length π. A variable time step is employed to obtain high accuracy during the spin-up phase and a CFL number less than 0.2 is guaranteed during the simulations. All the experiments run for $6 \cdot 10^5$ time steps. At each time step ψ is calculated from θ using a spectral method, variables being expanded as a sine series. ψ automatically satisfies the boundary conditions at $x = 0,\ \pi$ and $y = 0,\ \pi$ and

$$\widehat{\psi_{k,l}} = -\frac{1}{(k^2 + l^2)^{1/2}}\,\widehat{\theta_{k,l}}. \tag{15}$$

The Jacobian is finite differenced using a third-order upwinding scheme, which introduces an implicit friction term on θ of the form

$$\mu = U_{\max} (\Delta x)^3 \nabla^4 \psi_z, \tag{16}$$

where $U_{\max}$ is the maximum velocity at each time step and Δx is the grid space. This term helps to dissipate the enstrophy that builds up at small grid scales.

A_v is chosen to obtain the frictional boundary layer thickness between one and three grid points, in the physical range 2–$200\ \mathrm{cm^2\,s^{-1}}$. Of course when the nonlinear effects become important the thickness of the boundary layer is controlled by inertial effects.

We shall consider flows which have nonlinear and frictional effects of varying degrees, but our interest is in those flows which are strongly nonlinear, the linear case reproducing the same behavior of the linear homogeneous model. A measure of effects of nonlinearity is given by W and it can be modified by varying the value of the maximum wind stress τ_0.

The integrated equation is rescaled so that the coefficient arising from the

latitudinal variation in slope is $\Lambda = 1$ and (12) becomes

$$\partial_t \theta + J(\psi, \theta - y) = \nu \nabla^2 \psi + w' \operatorname{curl} \bar{\tau}, \tag{17}$$

where $w' = 1$ corresponds to a maximum wind stress $\tau_0 = 10^{-1}\,\mathrm{Nm}^{-2}$.

4·1. *Single-gyre configuration.* – Figure 1a-1d shows the streamfunction and the $(\psi_z - y)$ contours of a single gyre at different evolution times after reaching a statistically steady state, where steady means that after 10 integration time steps the maximum velocity and the mean square velocity differ by less than 1% from their previous values. The resolution is 512^2 grid points, ν is equal to 0.06 and w' is 2.

There is a north-south asymmetry produced by the northward advection of

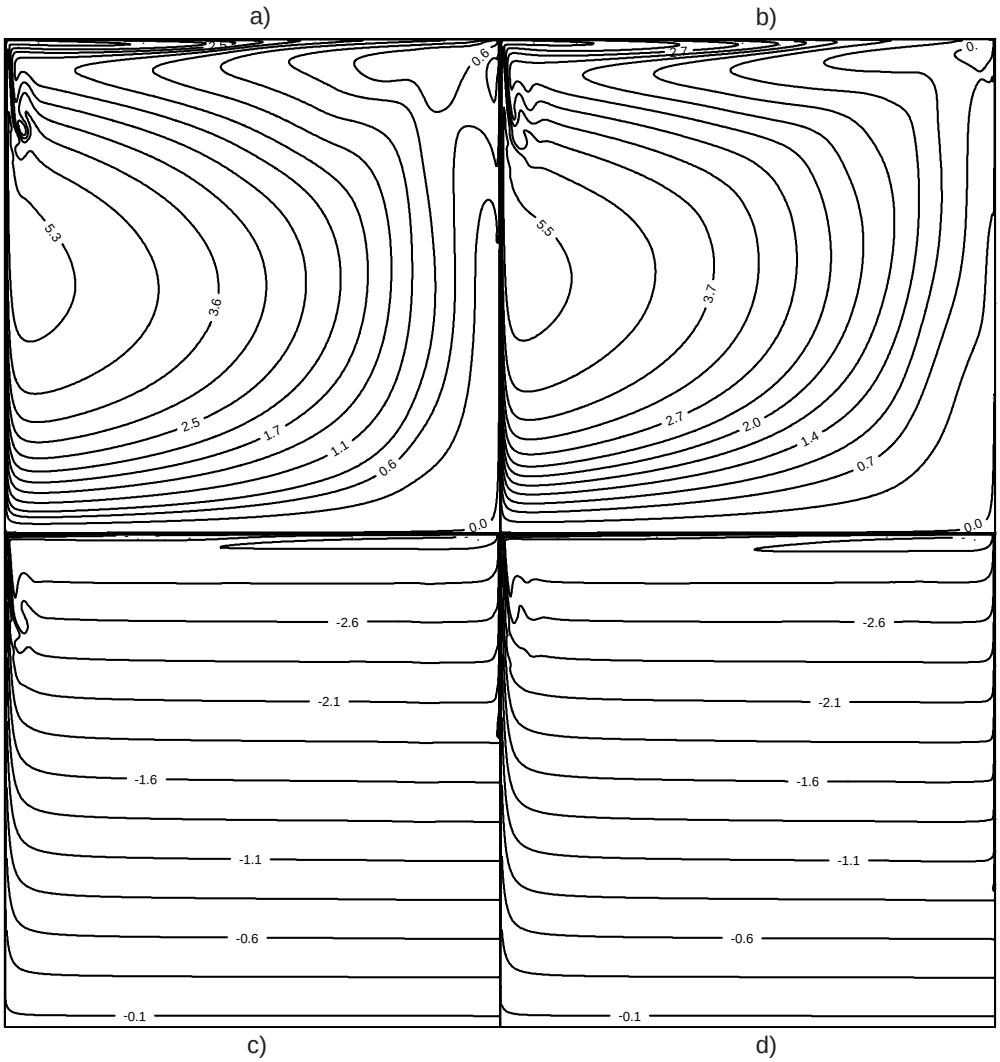

Fig. 1. – Evolution of a single-gyre configuration in the SQG model. a, b instantaneous ψ contours, c, d $\theta - y$ contours. $\tau_0 = 2 \cdot 10^{-1}\,\mathrm{Nm}^{-2}$, $A_v = 72\ \mathrm{cm}^2\,\mathrm{s}^{-1}$.

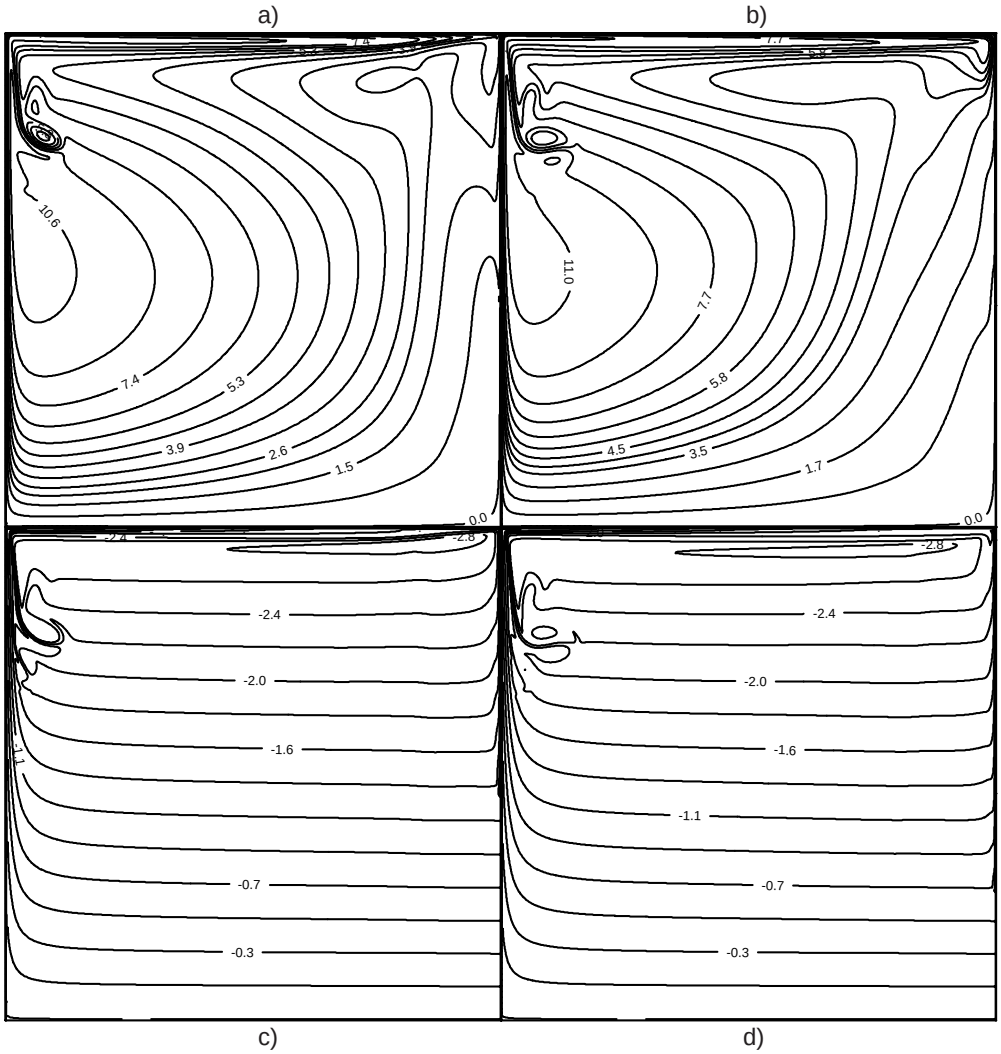

Fig. 2. – Evolution of a single-gyre configuration in the SQG model. a, b instantaneous ψ contours, c, d $\theta - y$ contours. $\tau_0 = 4 \cdot 10^{-1}\,\mathrm{Nm}^{-2}$, $A_v = 72\ \mathrm{cm}^2\,\mathrm{s}^{-1}$.

potential temperature. A thin, strong jet appears along the length of the northern wall. With the increasing of time (fig. 1b) the jet flows southward on the eastern boundary producing a weak eastern boundary current and modifing the interior configuration in the north. The nonlinear boundary current does not penetrate the interior except at the north-west corner, where a small recirculation zone is formed.

If inertial effects decrease in magnitude ($w' = 1$) and the inertial boundary thickness is of the same order of the frictional boundary, the jet along the northern wall becomes narrow and penetrates eastward slowly (not shown).

With ($w' = 4$) (fig. 2a-2b) the jet on the northern wall is broader. A stationary anticyclonic eddy forms before the flow joins the northern boundary and a recirculation

zone appears in the northeastern region (panel b), but there is no significant variation in the thickness of the western boundary, where most of the energy is confined.

We compared these results with simulations obtained by a classical homogeneous ocean model, where the flow is confined in a square, flat-bottomed basin, governed by the barotropic vorticity equation in the β-plane approximation and it is driven by the wind stress profile adopted in the SQG simulations with identical frictional retard.

As pointed out by Veronis [30], the complete neglect of horizontal friction is a singular perturbation of the vorticity equation. The integrated equation in the barotropic quasi-geostrophic model is

$$\partial_t q + J(\psi, q + \beta y) = - V \sin\left(\frac{\pi y}{L}\right) - \frac{E_v^{1/2}}{2R_0} \nabla^2 \psi , \tag{18}$$

where ψ is the two-dimensional streamfunction and q the potential vorticity ($q = \nabla^2 \psi$). In our nondimensional form $\beta = \frac{\beta_0 L^2}{U}$ and $V = \frac{\tau_0 L}{\varrho_s U^2 H}$, where H is the depth of the homogeneous layer and $\beta_0 = 2 \cdot 10^{-13}\,\mathrm{cm^{-1}\,s^{-1}}$.

In the rescaled form eq. (18) becomes

$$\partial_t q + J(\psi, q + y) = - v' \sin\left(\frac{\pi y}{L}\right) - \nu \nabla^2 \psi , \tag{19}$$

where $v' = 1$ corresponds to a maximum value of wind stress $\tau_0 = 10^{-1}\,\mathrm{Nm^{-2}}$ acting on a layer with depth 250 m.

With $v' = 1$ and $\nu = 0.06$, the flow evolving towards a statistically steady state is sufficiently nonlinear to resemble a Fofonoff free basin mode [33], which consists of a quasi-steady uniform westward interior flow closed by inertial boundary layers (not shown). Fofonoff flows, originally obtained for a barotropic configuration, assume a linear relation between the potential vorticity and the streamfunction, $q = a\psi + b$ with $a > 0$.

In the SQG model the eastward propagation of the current along the northern boundary is slower than in the homogeneous one because of the singular nature of the equations. In our SQG computation the fluid shoots across the entire northern wall in a thin boundary region, while in the interior the $(\psi_z - y)$ contours are parallel.

In the homogeneous model the maximum streamfunction in the domain measures the transport of the gyre quantifying the degree of spin-up [31]. If the interior is in linear Sverdrup balance, $\psi_{\max}$ would be unity in the particular case $v' = \beta = 1$. In the absence of lateral friction the interior streamfunction, rather than being predicted by the Sverdrup theory, is of the order of the rate between the inertial boundary thickness $\left(\frac{U}{\beta_0}\right)^{1/2}$ and the frictional boundary thickness $\frac{E_v^{1/2}}{2R_0\beta_0}$. In other words, in the single-gyre circulation the interior velocities exceed Sverdrup prediction in order to accomplish the necessary dissipation through the vertical friction.

In the SQG simulations with the same frictional coefficient and forcing the degree of spin-up is 1/6 of the value found in the homogeneous case. It means that the frictional terms (explicit and implicit) are more active in the SQG system in order to dissipate the energy accumulated at the western boundary and avoid the formation of a singularity.

4·2. *Double-gyre configuration.* – Figure 3a-3b shows the instantaneous ψ maps for a numerical simulation with $\nu = 0.01$, $w' = 2$ and a resolution of 512^2 grid points. In

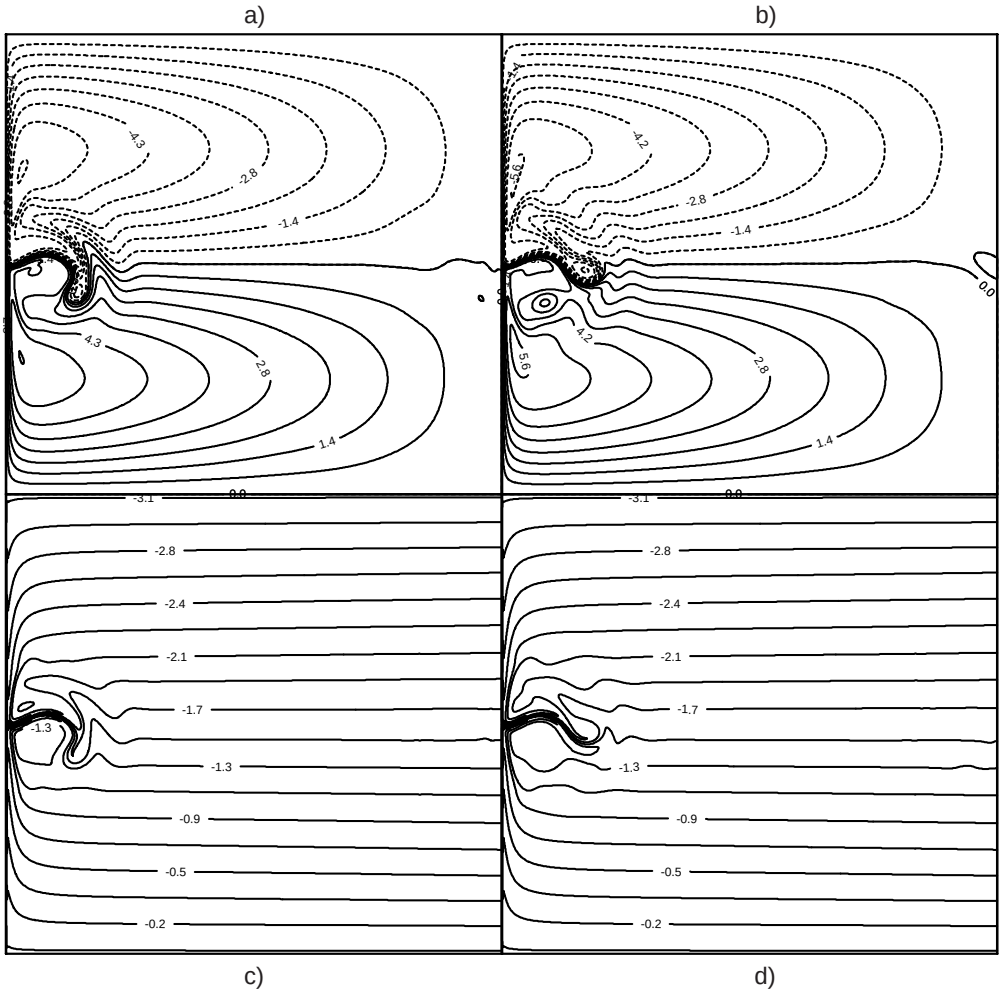

Fig. 3. – Evolution of a double-gyre configuration in the SQG model. a, b instantaneous ψ contours, c, d $\theta - y$ contours. $\tau_0 = 2 \cdot 10^{-1}\,\mathrm{Nm}^{-2}$, $A_v = 200\ \mathrm{cm}^2\,\mathrm{s}^{-1}$.

panel b the flow has already reached a statistically steady state. The western boundary currents south and north of the zero wind stress curl line become unstable at the ZWCL, forming a midlatitude short jet that penetrates eastward with a meandering movement. In the bends of the jet small eddies are formed and quickly destroyed by the high viscosity.

The circulation is dynamically unstable and in the double-gyre problem this leads to a degree of spin-up smaller than in the one-gyre case, because the vertical friction is coupled to lateral temperature exchange between the gyres. The difference between the two configurations (single and double gyre) is smaller than in the homogeneous case. The explanation is probably still in the character of the free waves propagation: the frictional contributions are almost of the same order to avoid the singularity formation which is independent of the wind stress symmetry.

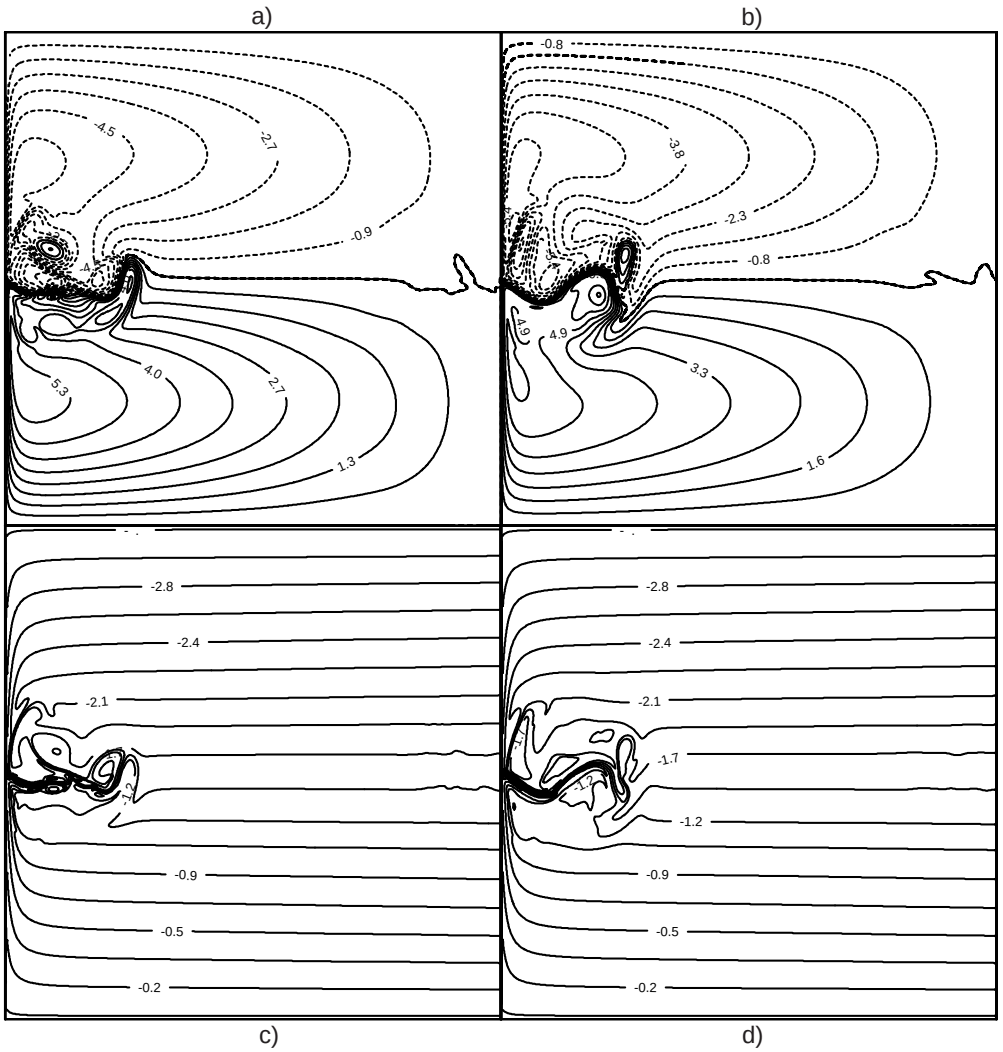

Fig. 4. – Evolution of a double-gyre configuration in the SQG model. a, b instantaneous ψ contours, c, d $\theta - y$ contours. $\tau_0 = 2 \cdot 10^{-1}\,\mathrm{Nm}^{-2}$, $A_v = 72\ \mathrm{cm}^2\,\mathrm{s}^{-1}$.

A region of recirculation exists in proximity of the ZWCL at the western wall where the isolines of total temperature are distorted. The $(\psi_z - y)$ contours (fig. 3c-3d) run west-east along latitude circles. At the western boundary they are attached to the western lateral wall. The flow must pass across $(\psi_z - y)$ contours from lower to higher values and in proximity of the midlatitude a region of significant recirculation is formed because of the strong gradients. The $(\psi_z - y)$ contours are not firmly attached to the west coast at their reference latitude $(-y)$. In a sufficiently nonlinear boundary current they can be drawn almost parallel to the streamlines.

In fig. 4 the forcing and the resolution are the same, but ν is equal to 0.006. When decreasing the viscosity coefficient, the nonlinear terms are dominant on the frictional

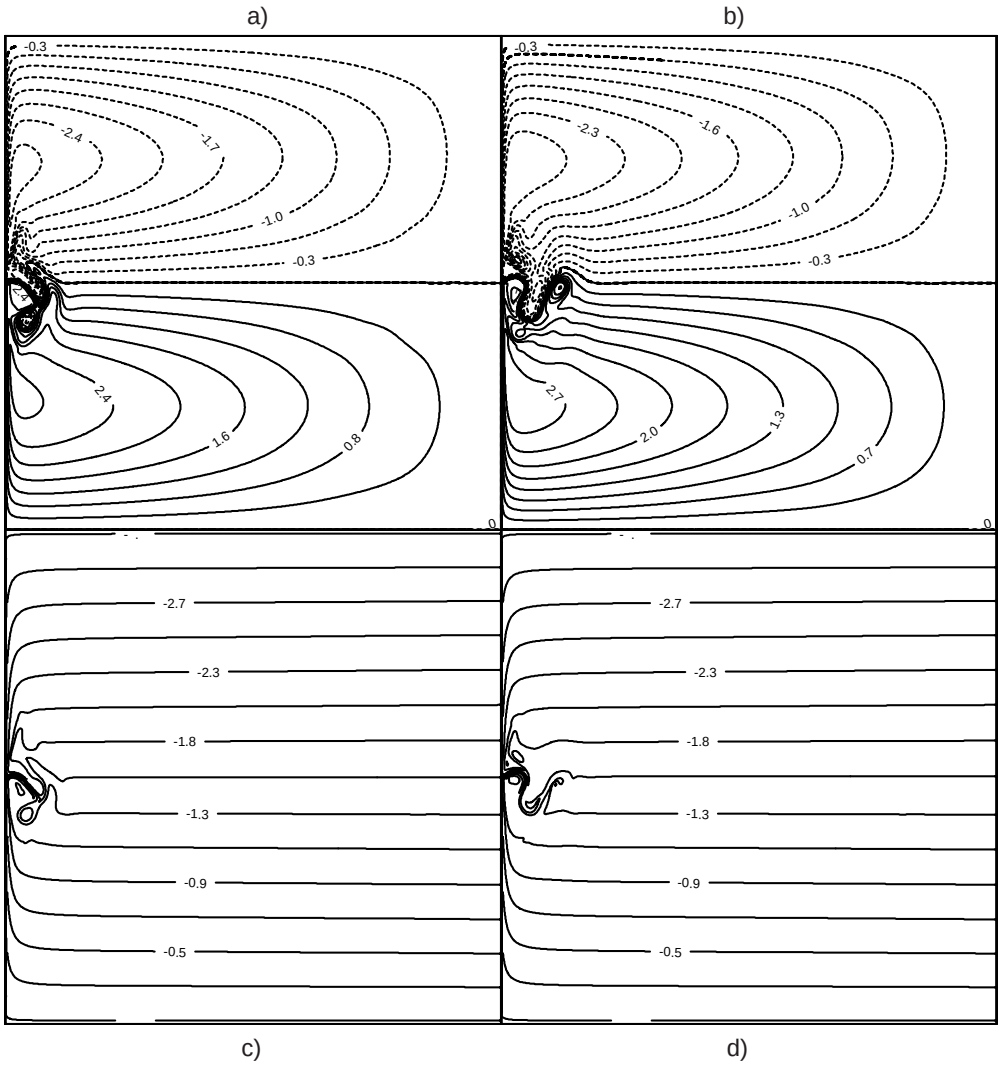

Fig. 5. – Evolution of a double-gyre configuration in the SQG model. a, b instantaneous ψ contours, c, d $\theta - y$ contours. $\tau_0 = 1 \cdot 10^{-1}\,\mathrm{Nm}^{-2}$, $A_v = 72\ \mathrm{cm}^2\,\mathrm{s}^{-1}$.

ones. The sensitivity of the solution to a small change in the bottom friction also indicates that the dissipation associated with the model's numerical scheme is minimal. The jet region appears elongated and the two recirculation zones north and south of the ZWCL are almost symmetric at the spin-up time (not shown). Evolving in time the recirculation zones increase and move north and south penetrating the interior with the formation of circular eddies not attached to the western boundary (panels a)-b)). In the SQG model the WBC is the region where the infinite-time singularity builds up with a front-like structure and no vortices can be created there. The eddies are generated just during the meandering motion of the jet at the separation latitude.

For $w' = 1$ and $\nu = 0.006$ (fig. 5a-5b) a strong circular anticyclonical eddy forms at

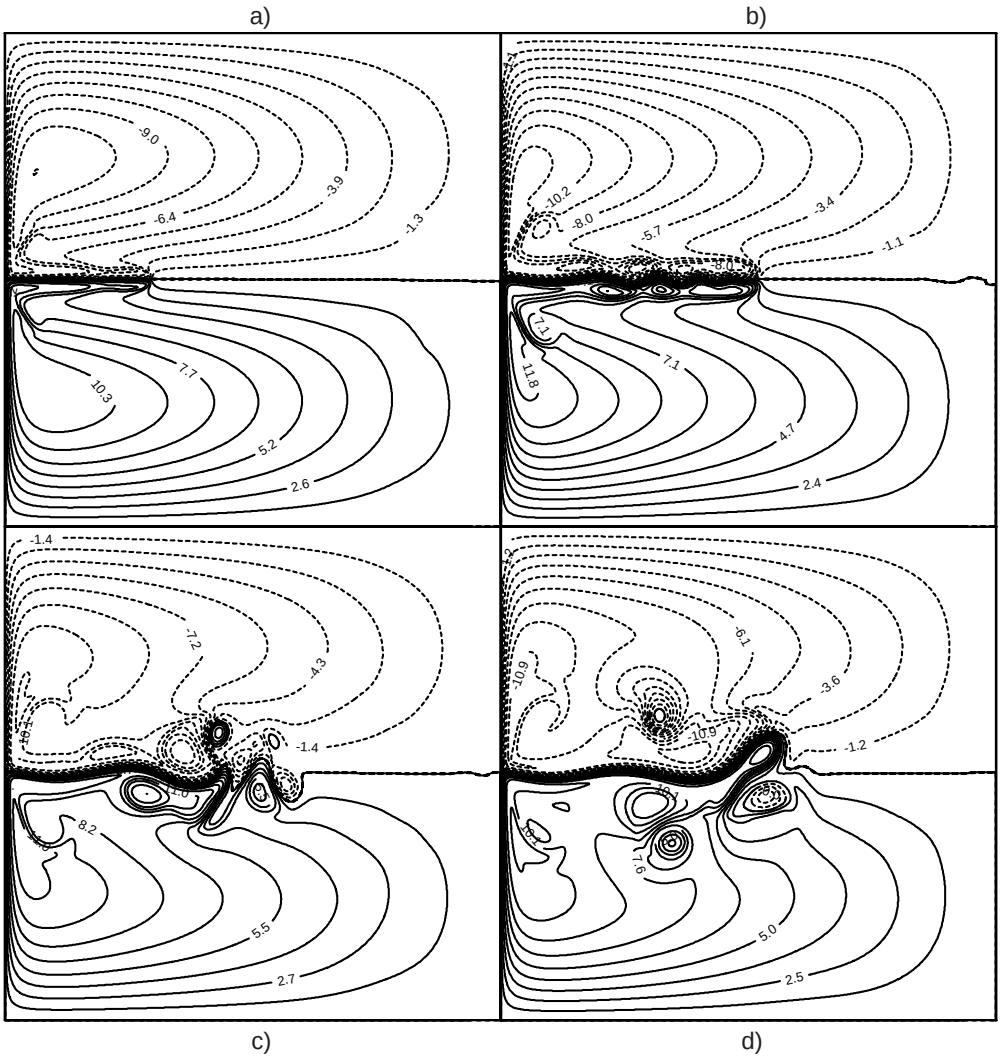

Fig. 6. – Evolution of a double-gyre configuration in the SQG model. a, d instantaneous ψ contours.

the midlatitude on the western boundary and slowly propagates eastward, surrounded by a thin and stretched cyclonical recirculation zone moving south. The ZWCL turns south following the cyclonical eddy and return at the midlatitude following the anticyclonical one. The jet now covers a small extent of the basin and its intensity decreases. The fluctuations of the jet are less violent and the resulting signature is weaker.

In fig. 6 $w' = 4$ and $\nu = 0.006$. In panels a) and b) the instantaneous streamfunction during the spin-up phase is presented; panels c) and d) show the flow when a statistically steady state is reached. There is a strong recirculation zone along the ZWCL with the formation of eddies that can easily penetrate the interior. The flow

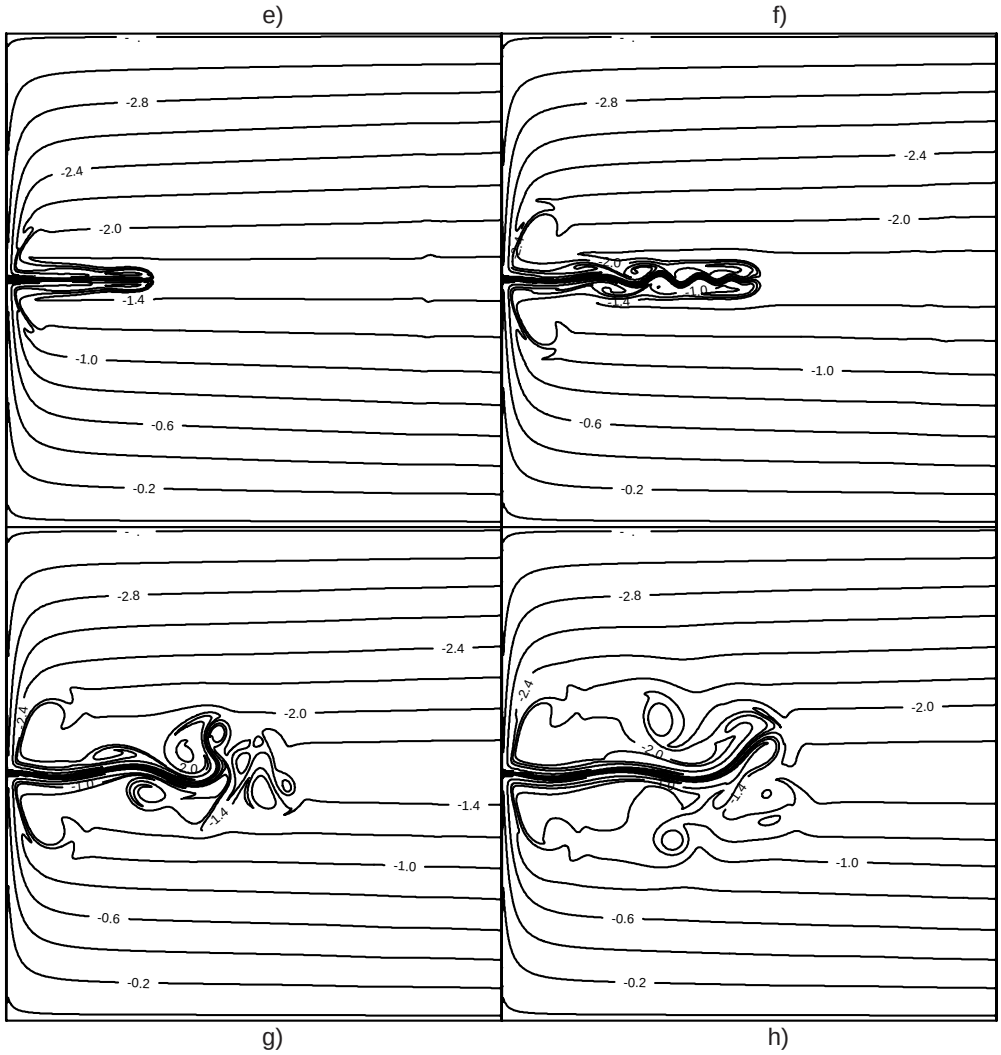

Fig. 6. – (*Continued.*) Evolution of a double-gyre configuration in the SQG model. e, h $\theta - y$ contours. $\tau_0 = 4 \cdot 10^{-1}\,\mathrm{Nm}^{-2}$, $A_v = 72\ \mathrm{cm}^2\,\mathrm{s}^{-1}$.

evolution shows the formation of complex structures with both cyclonical and anticyclonical eddies generated near the jet region that now covers more than half of the domain, as shown by the $(\psi_z - y)$ plots (fig. 6e-6h).

When increasing the resolution to 1024^2 grid points, with a viscosity coefficient $\nu = 0.001$ and $w' = 2$, complex recirculation zones appear surrounded by small-scale eddies propagating eastward slowly. This integration is not carried out to a perfect steady state. The primary difference from the previous experiment is that the midlatitude jet becomes more unstable with the production of a significant amount of small-scale activity in the region close to the jet. The jet now covers a small zonal extent of the basin. At the latest times (fig. 7b), the separation latitude moves to the south and

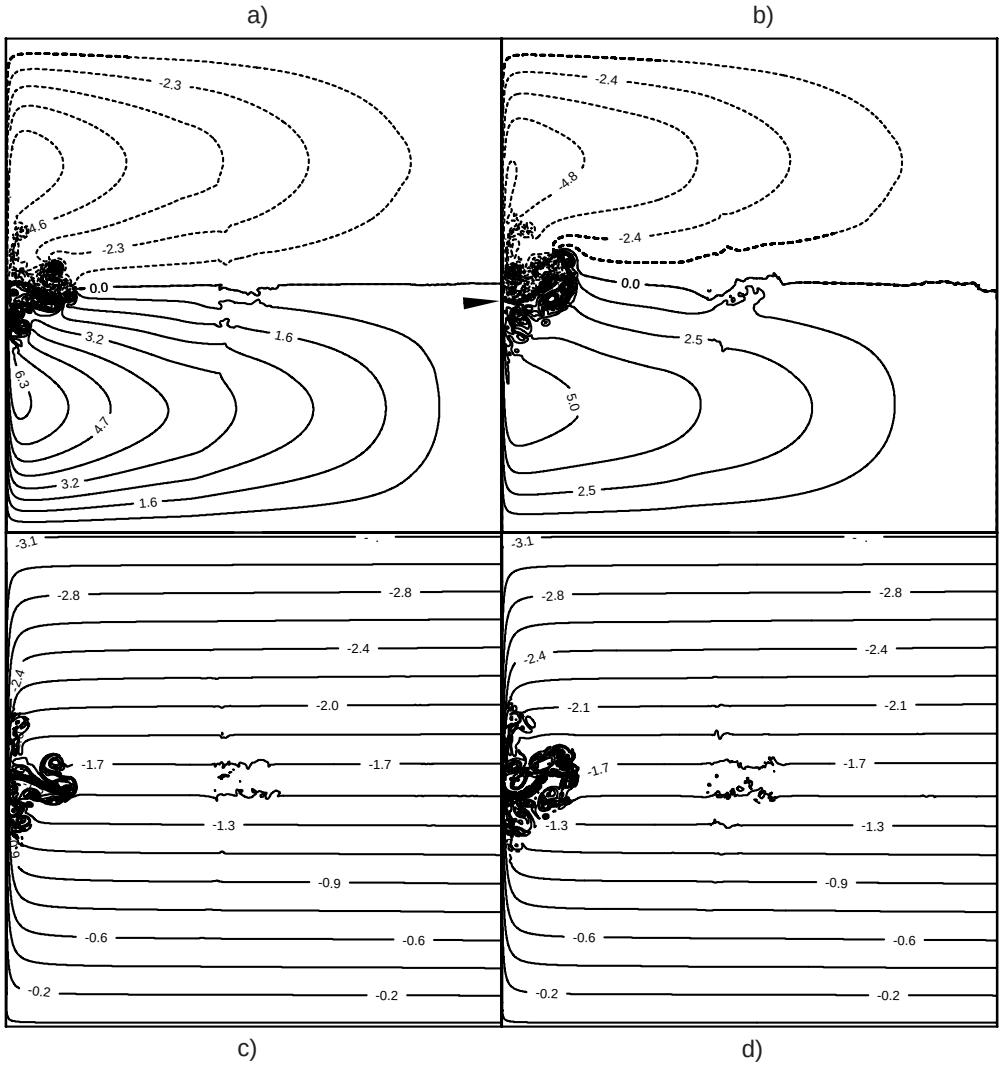

Fig. 7. – Evolution of a double-gyre configuration in the SQG model. a, b instantaneous ψ contours, c, d $\theta - y$ contours. $\tau_0 = 2 \cdot 10^{-1}\,\mathrm{Nm}^{-2}$, $A_v = 2\,\mathrm{cm}^2\,\mathrm{s}^{-1}$.

settles in approximately 40 km south of the ZWCL. This behavior is related to the decrease of bottom friction and is not observed in the previous simulation.

The scenario resulting from the single-layer quasi-geostrophic model is completely different. Equation (19) is integrated with a double-gyre wind stress profile with $v' = 0.4$ (fig. 8) and $\nu = 0.06$. The lateral viscosity coefficient is still set to zero. As shown by Griffa and Salmon [34] with an analogous model but with a different kind of viscosity, Fofonoff gyres do not emerge because the wind stress geometry opposes the Fofonoff flow.

A sample of the instantaneous streamfunction is presented in panel a) and the mean

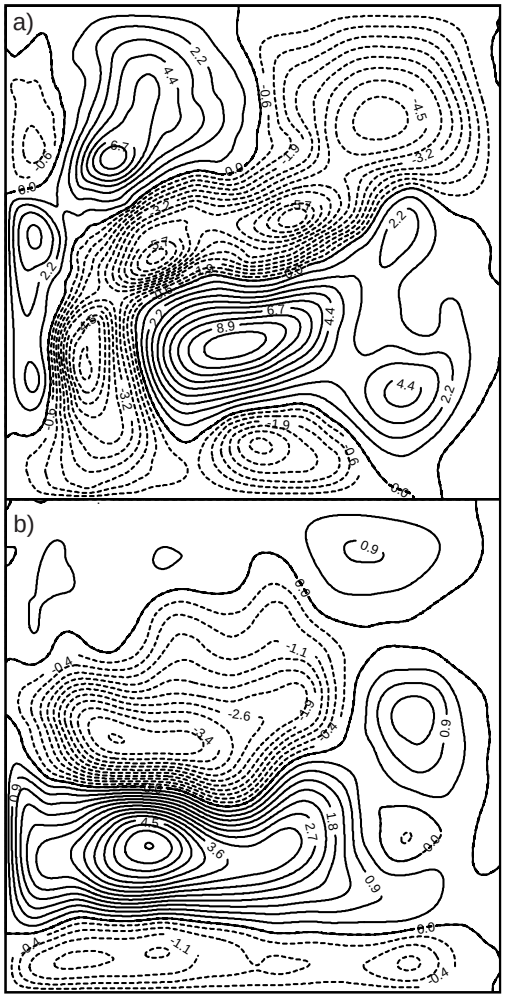

Fig. 8. – Evolution of a double-gyre configuration in the QG model. a instantaneous ψ contours, b mean streamfunctions. $\tau_0 = 4 \cdot 10^{-2}\,\mathrm{N m^{-2}}$, $A_v = 72\ \mathrm{cm^2\,s^{-1}}$.

streamfunction in panel b). A second set of gyres with opposite sign forms along the northern and southern boundary of the domain. These types of gyres are commonly observed in numerical simulations using the quasi-geostrophic approximation as well as primitive equation models [10, 12, 17]. The convergence of the western boundary current generates a midlatitude jet, but the mean signature is weaker than in the SQG case, and, by increasing the forcing, the penetration of the gyres in the domain decreases.

In the SQG model, the unidirectional propagation of the energy preserves the interior circulation in a Sverdrup balance and the only region where small-scale activity takes place is the jet extention. In the QG model when nonlinear interactions dominate, the short waves carry information to the east and the interior does not satisfy the Sverdrup relation.

5. – Conclusion

This study provides a particularly simple illustration of a wind-driven ocean circulation model where all the processes are driven by the dynamics of the upper boundary. Here a potential temperature field acts in the presence of a continuous stratification.

The SQG equations are integrated to study the dynamics in a closed basin. The linear form of the system is solved analytically, and the fully nonlinear time-dependent problem, with bottom friction and surface heating in the form of wind stress curl in single- and double-gyre configurations, is the subject of a numerical study. As for topographic waves propagating over a single vertical escarpment [28, 29, 35], the free waves are unidirectional and a singularity develops at infinite time along the western boundary. The waves propagate towards the western boundary and a thinning boundary layer forms together with a narrow jet of increasing velocity.

The simulations carried out were aimed at developing a new point of view to understand the current separation in the intergyre region without the usual assumption of a vertical discretization in a fixed number of layers of finite depth. As in the homogeneous model in the double-gyre configuration the circulation is dynamically unstable and extensive regions of recirculation and strong eddies form but, due to the singular nature of the SQG equation, they can propagate eastward slowly and they are created just in the jet region and not in the western boundary current. In the SQG model the frictional terms are more important than in the homogeneous one in order to dissipate the energy accumulated at the western wall. This leads to a small degree of spin-up both in the single- and the double-gyre cases. The bottom friction coefficient controls the separation latitude of the western boundary current: at high Reynolds number (smaller viscosity coefficient), the separation latitude moves south of the ZWCL. This behaviour is in agreement with the observations in the Gulf Stream.

The approximation of zero (or constant) potential vorticity at the interior is very strong. More realistic models must include planetary waves, the effects of a finite depth, a lateral viscosity. However, our results provide a further and simple illustration of the dynamical effects of waves often neglected, as for quasi-geostrophic calculations, that may have an important role on the ocean surface dynamics.

* * *

I gratefully acknowledge the support provided by the Woods Hole Oceanographic Institution Summer Student Fellowship program 1997 and all the GFD staff. Many thanks especially to Ted Johnson and Rick Salmon for ideas, discussions and the great encouragement: this work is the result of a summer project under their supervision.

REFERENCES

[1] HELD I. M, PIERREHUMBERT R. T., GARNER S. T. and SWANSON K. L., *Surface quasi-geostrophic dynamics*, *J. Fluid Mech.*, **282** (1995) 1.

[2] CESSI P., *Laminar separation of colliding western boundary currents*, *J. Mar. Res.*, **49** (1991) 697.

[3] CHASSIGNET E. P. and GENT P. R., *The influence of boundary conditions on midlatitude jet separation in ocean numerical models*, *J. Phys. Ocean.*, **21** (1991) 1290.

[4] Haidvogel D. B., McWilliams J. C. and Gent P. R., *Boundary current separation in a quasi-geostrophic, eddy-resolving ocean circulation model*, *J. Phys. Ocean.*, **22** (1992) 882.
[5] Holland W. R., *Baroclinic and topographic influences on the transport in western boundary currents*, *Geophys. Fluid Dyn.*, **4** (1973) 187.
[6] Thompson L., *The effect of continental rises on the wind-driven ocean circulation*, *J. Phys. Ocean.*, **15** (1995) 1296.
[7] Salmon R., *A two-layer model of Gulf Stream over a continental slope*, *J. Mar. Res.*, **50** (1992) 341.
[8] Salmon R., *Generalized two-layer models of ocean circulation*, *J. Mar. Res.*, **52** (1994) 865.
[9] Anderson T. L. D. and Killworth P. D., *Spin-up of a stratified ocean, with topography*, *Deep-sea Res.*, **24** (1977) 709.
[10] Verron J. and Le Provost C., *Response of eddy-resolved general circulation numerical models to asymmetrical wind forcing*, *Dyn. Atmos. Oceans*, **15** (1991) 505.
[11] Dengg J., *The problem of Gulf Stream separation: A barotropic approach*, *J. Phys. Ocean.*, **23** (1993) 2182.
[12] Özgökmen T. M., Chassignet E. P. and Paiva A. M., *Impact of wind forcing, bottom topography, and inertia on midlatitude jet separation in a quasi-geostrophic model*, *J. Phys. Ocean.*, **27** (1997) 2460.
[13] Thompson L. and Schmitz W. J. Jr., *A limited-area model of Gulf Stream: Design, initial experiments, and model-data intercomparison*, *J. Phys. Ocean.*, **19** (1989) 791.
[14] Spall M. A., *Dynamics of the Gulf Stream/deep western boundary current crossover. Part I: Entrainment and recirculation*, *J. Phys. Ocean.*, **26** (1996) 2152.
[15] Parson A. T., *A two-layer model of Gulf Stream separation*, *J. Fluid Mech.*, **39** (1969) 511.
[16] Veronis G., *Model of World Ocean circulation. Part I: Wind-driven, two-layer*, *J. Mar. Res.*, **31** (1973) 228.
[17] Chassignet E. P. and Bleck R., *The influence of layer outcropping on the separation of boundary currents. Part I: The wind-driven experiments*, *J. Phys. Ocean.*, **23** (1993) 1485.
[18] Chassignet E. P., Bleck R. and Rooth C. G. H., *The influence of layer outcropping on the separation of boundary currents. Part II: The wind- and buoyancy-driven experiments*, *J. Phys. Ocean.*, **25** (1995) 2404.
[19] Huang R. X., *A three-layer model for wind-driven circulation in a subtropical/subpolar basin. Part I: Model formulation and the subcritical state*, *J. Phys. Ocean.*, **17** (1987) 664.
[20] Pedlosky J., *The stability of currents in the atmosphere and in the ocean*, *J. Atmos. Sci.*, **21** (1964) 201.
[21] Charney J. G., *Geostrophic turbulence*, *J. Atmos. Sci.*, **28** (1971) 1087.
[22] Eady E. J., *Long waves and cyclonic waves*, *Tellus*, **1** (1949) 33.
[23] Blumen W., *Uniform potential vorticity flow: Part I. Theory of wave interactions and two-dimensional turbulence*, *J. Atmos. Sci.*, **35** (1978) 774.
[24] Anderson D. L. T. and Gill A. E., *Spin-up of a stratified ocean, with application to upwelling*, *Deep-Sea Reas.*, **22** (1975) 583.
[25] Constantin P., Nie Q. and Schörghofer N., *Nonsingular Surface-Quasi-Geostrophic flow. Phys. Lett. A*, **263** (1999) 15.
[26] Longuet-Higgins M. S., *Double Kelvin waves with continuous depth profiles*, *J. Fluid Mech.*, **34** (1968) 49.
[27] Rhines P. B., *Slow oscillations in an ocean of varying depth*, *J. Fluid Mech.*, **37** (1969) 161.
[28] Johnson E. R. *Topographic waves and evolution of coastal currents*, *J. Fluid Mech.*, **160** (1985) 499.
[29] Johnson E. R. and Davis M. K., *Free surface adjustment and topographic waves in coastal currents*, *J. Fluid Mech.*, **219** (1990) 273.

[30] VERONIS G., *Wind-driven circulation. Part II: Numerical solutions of the non-linear problem*, *Deep-Sea Res.*, **13** (1966) 31.
[31] PEDLOSKY J., *Geophysical Fluid Dynamics* (Springer-Verlag, New York) 1987, p. 710.
[32] STOMMEL H., *The westward intensification of wind-driven ocean currents*, *Trans. Am. Geophys. Union*, **29** (1948) 202.
[33] FOFONOFF N. P., *Steady flow in a frictionless homogeneous ocean*, *J. Mar. Res.*, **13** (1954) 254.
[34] GRIFFA A. and SALMON R., *Wind-driven ocean circulation and equilibrium statistical mechanics*, *J. Mar. Res.*, **47** (1989) 457.
[35] PAGE M. A. and JOHNSON E. R., *Nonlinear western boundary current flow near a corner*, *Dyn. Atmos. and Oceans*, **15** (1991) 477.